

Identification of Kinetics of Direct Esterification Reactions for PET Synthesis Based on a Genetic Algorithm

Ju-Youl Kim, Hee-Young Kim* and Yeong-Koo Yeo†

Department of Chemical Engineering, Hanyang University,
17 Haengdang-dong, Sungdong-ku, Seoul 133-791, Korea

*Korea Research Inst. of Chemical Technology, Yusong, Daejeon 306-600, Korea

(Received 2 May 2001 • accepted 15 June 2001)

Abstract—In this study we propose a method to identify the kinetics of direct esterification reactions for polyethylene terephthalate (PET) based on a genetic algorithm. The reaction rate parameters could be identified successfully by using a genetic algorithm and plant data. The effects of key operating variables (temperature, pressure, monomer feed ratio and residence time) on the reactor performance were also investigated. It was observed that the reactor performance strongly depends on the degree of dissolution of the solid terephthalic acid (TPA) in the reaction mixtures.

Key words: Direct Esterification, Polymerization Reactor Modeling, Reaction Rate Parameters, Genetic Algorithm

INTRODUCTION

PET can be manufactured by using either dimethyl terephthalate (DMT)-ethylene glycol (EG) or terephthalic acid (TPA)-EG as raw materials [Kumar et al., 1984]. Fig. 1 shows a typical continuous PET synthesis process that consists of five reactors. The vapor resulting from each reactor passes through recovery equipment including a distillation tower and a spray condenser from which excess EG is separated from water-EG vapor mixture and is recycled. The process mainly consists of two sections: esterification section and polymerization section. The esterification section in turn consists of the primary and secondary esterification reactor, and the polymerization section consists of three polymerization reactors: a continuous stirred tank reactor, a single-shafted horizontal polymer finishing reactor and a double-shafted horizontal finishing reactor.

Due to long reaction time, high reaction temperature and multi-level production facilities with large capacity, the PET production process is highly energy intensive process. In particular, the amount of energy required in the primary esterification reactor is very large compared with successive reactors in a continuous process [Yamada, 1992]. Furthermore, the disposal of the heat medium waste discharged from the process has been a troubling issue. Therefore, it is necessary to analyze the first esterification process in detail in order to reduce heat injection and to decrease the production cost.

In the direct esterification reactor diethylene glycol (DEG) is the most important side product. The DEG production reaction is the governing side reaction in the early stages of PET synthesis, while other side products (acetaldehyde, vinyl end groups, etc.) are formed mainly in the final stages of polycondensation [Ravindranath and Mashelkar, 1986]. The amount of DEG in PET molecules influences the physical and chemical properties of the polyester. For instance, the melting point of PET is lowered by about 5 °C for every percentage unit (by weight) of DEG content [Hovenkamp and Munting, 1970], and when DEG content increases thermal transitions

(T_g , crystallization temperature) are decreased linearly [Besnoin and Choi, 1998]. The exact prediction of DEG concentration in the reaction mixtures is very important in the modeling of a reactor.

The DEG formation mechanisms are very complex [Besnoin and Choi, 1989]. DEG exists in the forms of terminal DEG, bound DEG and free DEG. For these reasons it is difficult to measure DEG formation kinetics. Several studies [Yamada, 1992; Ravindranath and Mashelkar, 1982; Immanuel and Gupta, 2000; Kang et al., 1997] on the modeling, simulation and optimization of the continuous direct esterification stage of PET polymerization process have been reported. Previous models employed some abbreviation or simplification by various assumptions to represent the kinetics. Hence the exact evaluation of DEG production kinetics is essential before modeling and simulation studies.

Estimation of rate constants of complex reaction schemes is often related to compromises between the desired detailed mathematical description by rate equations being meaningful from a chemical and physicochemical point of view and the computational limitations in handling the size and nonlinearity of such models [Wolf and Moros, 1997]. Genetic algorithms (GAs) could be a potential tool for finding initial estimates in large parameter spaces since many different solutions are investigated and refined simultaneously to identify near-optimum solutions so far. In recent years, GAs have been applied to analyze unknown and nonlinear chemical kinetics. Wolf and Moros [1997] and Park and Froment [1998] have analyzed the rate and certainty of convergence of genetic algorithms illustrating some applications to a nonlinear kinetic model of the heterogeneous catalytic reactions. Polifke et al. [1998] used GAs to determine optimum rate coefficients of simplified kinetic mechanisms by matching heat release and species production rates. Harris et al. [2000] used GAs to predict reaction rate parameters into modified Arrhenius form. The results of these investigations have proved that GAs could be effectively used to assess the behaviors of complex reactions where the reaction rate coefficients are not known with any confidence. The basic concept of GAs was first conceived by Holland [1975] and has been developed by Davis [1987], Goldberg [1989] and Michalewicz [1996]. GAs were employed to de-

†To whom correspondence should be addressed.
E-mail: ykyeo@email.hanyang.ac.kr

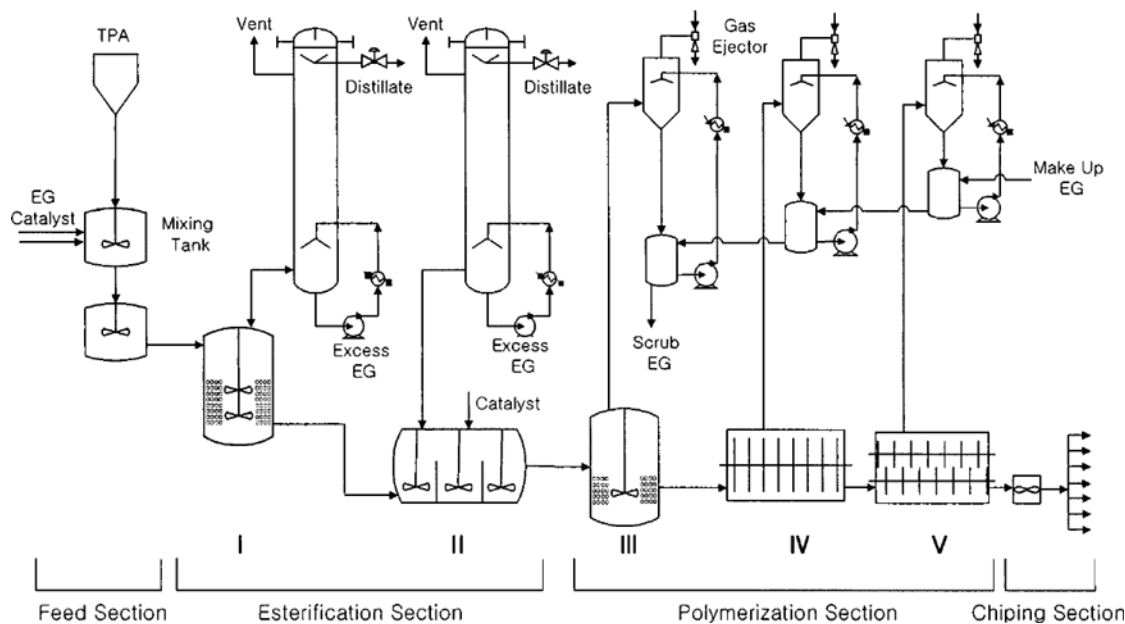


Fig. 1. Schematic of continuous PET synthesis process.

velop optimization techniques based on the principles of natural genetics and natural selection.

In optimizations, GAs begin to work with a population of solutions instead of a single solution, and use probabilistic rules to determine search directions. GAs also use a coding of variables (genotype space) instead of variables themselves (phenotype space). GAs are very efficient and robust in finding global optima regardless of the types of optimization problems: discrete or nonlinear [Deb, 1996]. Most polymer synthesis processes exhibit complex and nonlinear behaviors, and a GA is a quite appropriate choice to solve optimization problems related to polymer processes.

In the present study we first developed a model for a PET production plant. Basic modeling techniques for the actual plants can be utilized in the present study [Yeo et al., 1996, 1998]. The basic structure of the model proposed in the present work is similar to that of Kang et al. [1997], where the required kinetic data of DEG production reaction rely on the results of Reimschuessel's experiments [1979] and those of other reactions on the results of Otton and Ratton's experiments [1998]. Such incorrect and impractical data may cause serious errors in the analysis of reaction processes. We analyzed the reaction rate parameters of DEG production through the comparison of original plant data with calculated data by using a simple genetic algorithm (SGA). To the author's knowledge, to date, no application results of GAs in the determination of the kinetics of polymerization processes by original plant data have been reported so far. The reaction kinetics obtained were used in turn to identify conversion of acid end groups, degree of polymerization and the concentration of by-products rates according to the change of operating conditions.

MODELING OF THE ESTERIFICATION REACTOR

In the modeling of a direct esterification reactor, we first assumed that polymerization reactions involved can be regarded as reactions

between two functional groups and that the reactivity of a functional group does not depend on the polymer chain length because of the relatively low the degree of polymerization (DP) of the direct esterification product [Flory, 1953]. These assumptions enable us to regard all reactions in the reactor to occur by polymer segments. Related reactions among these polymer segments and simplified kinetic schemes of esterification stages are summarized in Table 1. The reactions in Table 1 are identical to the six reactions of Kang et al. [1997]. In Table 1, the first four reactions are esterifi-

Table 1. Reaction schemes of functional groups in the direct esterification stages of the PET synthesis process (t-: terminal, b-: bound)


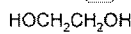

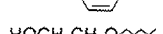
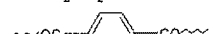
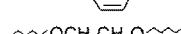
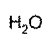
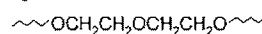
Reaction scheme	
Esterification reactions	$\text{TPA} + \text{EG} \xrightleftharpoons[k_d/k_r]{k_f} \text{t-TPA} + \text{t-EG} + \text{W}$ $\text{t-TPA} + \text{EG} \xrightleftharpoons[k_d/k_r]{k_f} \text{b-TPA} + \text{t-EG} + \text{W}$ $\text{TPA} + \text{t-EG} \xrightleftharpoons[k_d/k_r]{k_f} \text{b-EG} + \text{t-TPA} + \text{W}$ $\text{t-TPA} + \text{t-EG} \xrightleftharpoons[k_d/k_r]{k_f} \text{b-EG} + \text{b-TPA} + \text{W}$
Polymerization reactions	$\text{t-EG} + \text{t-EG} \xrightleftharpoons[k_d/k_r]{k_p} \text{b-EG} + \text{EG}$
Side reaction (DEG formation)	$\text{t-TPA} + \text{EG} \xrightarrow{k_s} \text{b-DEG} + \text{W}$
Molecular structures of components	
TPA	Terephthalic acid 
EG	Ethylene glycol 
t-TPA	TPA end group 
t-EG	EG end group 
b-TPA	Bound TPA 
b-EG	Bound EG 
W	Water 
b-DEG	Bound DEG 

Table 2. Reaction rate parameters and equilibrium constants for reactions in Table 1 (C_{acid} : the concentration of acid end groups in the liquid phase, k_1 - k_5 : from Otton and Ratton's experiments [1989])

Kinetic constants $k_i = A_i C_{acid} \exp(-E_i/RT)$	Activation energy E_i [cal/mol]	Frequency factor A_i [(kg/mol) ² /min]	Equilibrium constant K_i
k_1	180000	6.2974×10^5	2.50
k_2	180000	6.2974×10^5	2.50
k_3	180000	3.1487×10^5	1.25
k_4	180000	3.1487×10^5	1.25
k_5	180000	4.8980×10^5	0.50
$k_6 = A_6 \exp(-E_6/RT)$			

Table 3. Equilibrium data used for modeling of a direct esterification reactor

Phase equilibrium	
Vapor-Liquid Equilibrium	$P_i = P_r \cdot y_i = P_i^{sat} \cdot x_i$, $P_r = P_{EG} + P_{H_2O}$ $\ln P_{EG}(pa) = 79.3 + (-10105/T) + (-7.5 \ln T) + 7.3 \times 10^{-10} \times T^6$ $\ln P_w(pa) = 73.6 + (-7259/T) + (-7.3 \ln T) + 4.2 \times 10^{-6} \times T^2$
Solid-Liquid Equilibrium	$\alpha = \alpha_{EG} \omega_{EG}^0 + \alpha_{OLG} \omega_{OLG}^0 + \alpha_w \omega_w^0 = \alpha_{EG} \omega_{EG}^0 + \alpha_{BHEET} \omega_{OLG}^0$ $\alpha_{EG}(\text{dissolved TPA mol/EG 1 kg}) = 9062 \exp(-4877/T)$ $\alpha_{BHEET}(\text{dissolved TPA mol/OLG 1 kg}) = 374 \exp(-3831/T)$
Density of reaction mixtures (ρ) = 1.160 kg/l	

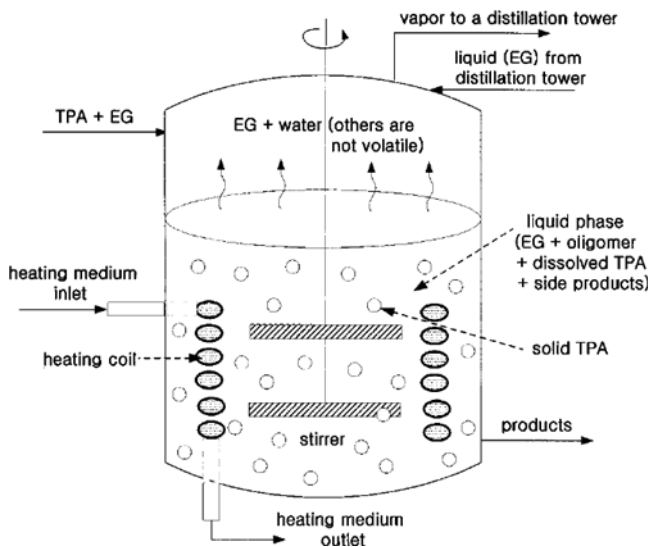
cation reactions, the fifth reaction is the polymerization reaction, and the sixth reaction is the DEG production reaction which is the governing side reaction in the early stages of PET synthesis. Reactions from 1st to 5th are acid-catalyzed reactions.

The reaction mixture in the direct esterification reactor is a heterogeneous system in which solid, liquid and vapor phases are jumbled together. Due to the solid TPA, a monomer in PET synthesis has very low solubility in EG. Solid and liquid phase equilibrium and the mean solubility of TPA in the reaction mixtures are the key factors that describe the complicated reaction system. The mean solubility of TPA is calculated by using experimental data by Yamada et al. [1985], which were compared and verified with previous solubility data. Vapor and liquid phase equilibrium can be calculated from Raoult's law. This approach is justified by the high temperature and low pressure in the actual operation of the PET plant. Table 2 shows kinetic and equilibrium data for reactions in Table 1, and Table 3 shows phase equilibrium relations for both vapor-liquid and solid-liquid.

Fig. 2 is a simple schematic of the reaction system in the direct esterification reactor. As shown in Fig. 2, it is assumed that the vapor pressure is contributed only by EG and water because oligomer is not volatile, the vapor pressure of TPA and DEG are negligible, and only EG vapor is recycled completely. All reactions proceed in the liquid phase, and the density of the reaction mixtures is assumed to be constant. Even though the reaction mixtures are slurry with high viscosity, the assumption of perfect mixing in the esterification reactor is reasonable since various mixing units are used in the actual plant to prevent loss due to imperfect mixing.

Steady-state mass balances for all components can be written based on the assumptions and effective rate constants including the effect of acid catalyst.

$$F + F^R = F^C + F^V \quad (1)$$

**Fig. 2. Schematic of a direct esterification reactor in PET synthesis.**

$$W_{mix} (dC_{TPA}^c/dt) = F^c C_{TPA}^c - F^c C_{TPA}^o + W \{-R_1 - R_3\} = 0 \quad (2)$$

$$W_{mix} (dC_{EG}^c/dt) = F^c C_{EG}^c - F^c C_{EG}^o + W \{-R_1 - R_3 + R_5\} - F^R C_{EG}^R - F^R C_{EG}^R = 0 \quad (3)$$

$$W_{mix} (dC_{T-TPA}^c/dt) = F^c C_{T-TPA}^c - F^c C_{T-TPA}^o + W \{R_1 - R_2 + R_3 - R_4\} = 0 \quad (4)$$

$$W_{mix} (dC_{T-EG}^c/dt) = F^c C_{T-EG}^c - F^c C_{T-EG}^o + W \{R_1 + R_2 - R_3 - R_4 - 2R_5 - 2R_6\} = 0 \quad (5)$$

$$W_{mix} (dC_{b-TPA}^c/dt) = F^c C_{b-TPA}^c - F^c C_{b-TPA}^o + W \{R_2 + R_4\} = 0 \quad (6)$$

$$W_{mix} (dC_{b-EG}^c/dt) = F^c C_{b-EG}^c - F^c C_{b-EG}^o + W \{R_3 + R_4 + R_5\} = 0 \quad (7)$$

$$W_{mix} (dC_w^c/dt) = F^c C_w^c - F^c C_w^o + W \{R_1 + R_2 + R_3 + R_4 + R_5\}$$

$$-F^v C_w^v + F^s C_w^s = 0 \quad (8)$$

$$W_{mix} (dC_{b-DEG}^c / dt) = F^c C_{b-DEG}^c - F^o C_{b-DEG}^c + W \{R_6\} = 0 \quad (9)$$

where

$$R_1 = 4k_1 C_{TBA} C_{EG} - (k_1/K_1) C_{TBA} C_w \quad (10)$$

$$R_2 = 2k_2 C_{EG} C_{TBA} - 2(k_2/K_2) C_{b-TBA} C_w \quad (11)$$

$$R_3 = 2k_3 C_{T-EG} C_{TBA} - (k_3/K_3) C_{T-TBA} C_w \quad (12)$$

$$R_4 = k_4 C_{T-EG} C_{T-TBA} - 2(k_4/K_4) C_{b-TBA} C_w \quad (13)$$

$$R_5 = k_5 C_{T-EG}^2 - 4(k_5/K_5) C_{b-EG} C_{EG} \quad (14)$$

$$R_6 = k_6 C_{T-EG}^2 \quad (15)$$

IDENTIFICATION OF REACTION RATE PARAMETERS

In order to obtain reliable values of the DEG reaction rate parameters of the present model, we introduced an error function given by

$$E(x) = \sum_i \left(\frac{P_{i,calc} - P_{i,plant}}{P_{i,calc}} \right)^2 \times 10^n \quad (16)$$

where

P: vector of product properties

x: vector of reaction rate parameters

The flow rate of water and EG vapor and the concentration of acid end groups are key properties to be analyzed in the present study. Other properties such as the concentration of DEG, the degree of polymerization and so forth could not be checked due to lack of operation data. The flow rate of water vapor is affected by esterification reactions and depends considerably on the DEG formation mechanism. Therefore the concentration of DEG can be represented in terms of the water vapor rate. In the same manner, the degree of polymerization (namely the degree of all reactions in the reactor) can be included in the concentration of acid end groups, and the flow rate of EG and water vapor can be used to describe the degree of esterification, polycondensation and DEG production reaction. The objective function for the optimization based on these facts and the error function can be constructed as

$$\text{Minimize } I(x) = \sum \left[\left(\frac{F_{EG,calc}^v - F_{EG,plant}^v}{F_{EG,calc}^v} \right)^2 + \left(\frac{F_{w,calc}^v - F_{w,plant}^v}{F_{w,calc}^v} \right)^2 + \left(\frac{C_{acid,calc}^c - C_{acid,plant}^c}{C_{acid,calc}^c} \right)^2 \right] \times 10^4 \quad (17)$$

The rate constant for DEG formation reaction is shown in Table 2. The decision variables vector **x** in (17) consist of A_6 and E_6 (frequency factor and activation energy of the sixth reaction in the Table 2). The ranges of these variables are

$$1.0 \times 10^8 \leq A_6 \leq 5.0 \times 10^8, 2.0 \times 10^4 \leq E_6 \leq 4.0 \times 10^4 \quad (18)$$

Determining the ranges of decision variables is very important because incorrect ranges can give an undesirable combination of

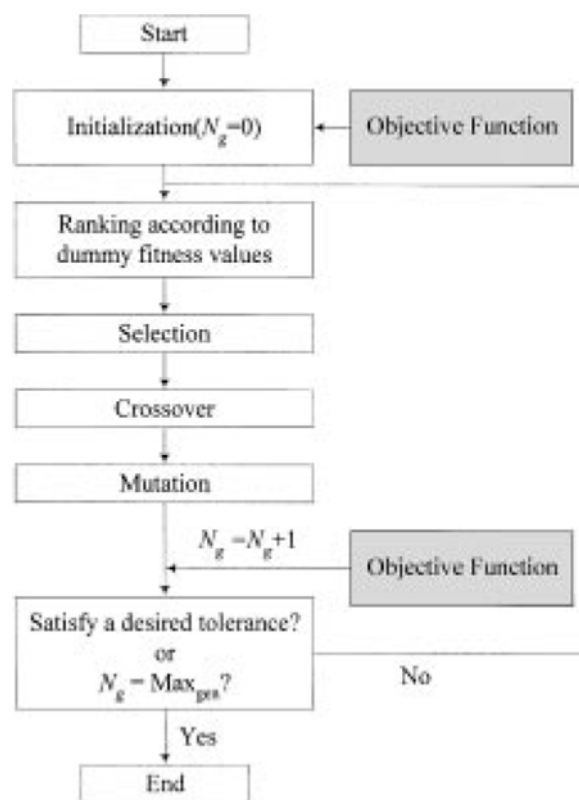


Fig. 3. Flowchart of the genetic algorithm used in the present study.

kinetic parameters, which results in failure in the modeling. The ranges given by (18) were obtained empirically after preliminary trials by using the reaction rate parameters of DEG formation reaction and various simulation results.

In order to successfully identify all the reaction rate parameters, we utilized the genetic algorithm technique for the optimization. Fig. 3 shows a flowchart of the GA used in this work. The first step in the GA procedure consists of determination of strategies about encoding type, reproduction, crossover, mutation and sharing, followed by selection of the value of parameters for the GA employed. To initialize a population, we can simply set a number of chromosomes randomly in bitwise fashion. The length of these binary-encoded strings is usually determined according to the desired solution accuracy. We used 32-bit coding for a variable in this paper. Genes of each chromosome represent encodings of all the unknown reaction rate parameters over some specified ranges. Each chromosome in genotype space is decoded to the real value of each individual, and then all fitness values of these individuals for an objective function are obtained by using a proper model, which can describe the real behaviors of a target system well. In this work the fitness function value was calculated according to the accuracy of the net properties about reactor performance against some known real plant measurements.

The reproduction process makes good strings in a population assigned probabilistically a larger number of copies, and so a mating pool is formed. We employed a stochastic remainder selection scheme [Deb, 1996], which uses the idea of ranking selection [Goldberg, 1989] for a reproduction operator. The ranking selection method keeps appropriate levels of selection pressure throughout simu-

lations. A rank is assigned to each string with values of 1 (best) to N (worst) according to the fitness function value. Next, stochastic remainder roulette wheel selection is operated until the mating pool is full of the better strings according to the rule that copies exactly equal to the mantissa of the expected count (dummy fitness value divided by the average dummy fitness value) are first assigned to the strings. The regular roulette-wheel selection is then implemented by using the decimal part of the expected count as the probability of selection [Deb, 1996].

The main purpose of the crossover operator (P_c) is to search the parameter space and to perform in a way to preserve the information stored in the parent strings maximally. We have selected two point crossover and $P_c=0.8$, which makes two reproduced parent strings exchange inner part between two random crossover points

Table 4. The parameters of genetic algorithm used

Maximum generation number, Max_{gen}	100
Population size, N_p	50
Crossover operator, P_c	0.8
Random number, seed	0.5
Number of decision variables, N_d	2
Chromosome length, l_{chrom}	32
Mutation operator, P_m	0.001

with the probability of 0.8. Mutation operator (P_m) maintains diversity in the population in such a way that all bits in each string are changed from 1 to 0 and vice versa with a given mutation probability. We have chosen $P_m=0.001$ because a small mutation opera-

Table 5. Comparison between the plant operation data and the simulation results by using the calculated parameters for DEG formation reactions

No	Reactor conditions				Reactor properties				
	T (°C)	P (atm)	τ (hr)	a		$F_{EG}^v(-)$	$F_{water}^v(-)$	$C_{acid}^o(-)$	
1	260	1.2383	3.3277	1.2100	Plant	0.1421	0.1835	0.3248	
					Calculated	0.1426	0.1849	0.3318	
	259	1.2383	3.3228	1.2422	Plant	0.1435	0.1846	0.3237	
					Calculated	0.1434	0.1865	0.3191	
	259.9	1.2383	3.3388	1.2518	Plant	0.1467	0.1893	0.3082	
					Calculated	0.1438	0.1870	0.3089	
	260	1.2383	3.3472	1.2800	Plant	0.1668	0.1902	0.2948	
					Calculated	0.1670	0.1891	0.2941	
	26.3	1.2383	3.1729	1.3425	Plant	0.2056	0.1890	0.2769	
					Calculated	0.2059	0.1914	0.2771	
260	1.2383	3.2159	1.3504	Plant	0.2117	0.1897	0.2747		
				Calculated	0.2118	0.1917	0.2742		
2	259	1.1125	3.9807	1.2288	Plant	0.1565	0.1907	0.2898	
					Calculated	0.1558	0.1900	0.2905	
	259	1.1416	3.8357	1.2246	Plant	0.1492	0.1915	0.2999	
					Calculated	0.1475	0.1887	0.2985	
	259	1.1706	3.8836	1.2204	Plant	0.1408	0.1842	0.3062	
					Calculated	0.1422	0.1883	0.3012	
3	259	1.1899	3.4612	1.2309	Plant	0.1426	0.1842	0.3085	
					Calculated	0.1437	0.1871	0.3086	
	259	1.1899	3.6677	1.2351	Plant	0.1435	0.1878	0.2984	
					Calculated	0.1449	0.1879	0.3034	
	259	1.1125	3.9807	1.2288	Plant	0.1565	0.1907	0.2898	
					Calculated	0.1558	0.1900	0.2905	
	259	1.1899	4.3825	1.2403	Plant	0.1451	0.1905	0.2829	
					Calculated	0.1475	0.1903	0.2876	
	4	259	1.1416	3.8014	1.2426	Plant	0.1582	0.1868	0.2919
						Calculated	0.1584	0.1896	0.2921
259		1.1899	3.7829	1.2397	Plant	0.1483	0.1835	0.2941	
					Calculated	0.1500	0.1887	0.2976	
259		1.2090	4.0225	1.2403	Plant	0.1519	0.1901	0.2926	
					Calculated	0.1521	0.1896	0.2924	
259		1.2383	3.5076	1.2422	Plant	0.1458	0.1883	0.3084	
					Calculated	0.1448	0.1873	0.3072	

tor is used generally. Table 4 summarizes typical GA parameters used in the present study. One cycle of the genetic algorithm is composed of these procedures as described above. The cycle is repeated until objective values of all individuals shrink to a desired tolerance or the number of generation approaches a prespecified maximum number. In Fig. 3 the objective function represented by gray blocks includes the esterification reactor model.

RESULTS AND DISCUSSION

The actual plant operation data can be effectively used to verify the plant model developed. Usually the operation data are dispersed over a certain limited region. For the purpose of modeling and analysis, it is most convenient to classify the operation data into several types of sets [Bhaskar et al., 1999]. In this work four sets of operating data as shown in Table 5 were used in the verification of the model developed.

In the first data set feed mole ratios (EG/TPA) are different mutually, while other conditions are virtually the same with each other. Therefore, this set can be used to show the effects of the feed mole ratio on the reactor performance. The range of the feed mole ratio was from 1.21 to 1.35. In the same manner, the second data set can be used to prove the effects of pressure of which the range is from 1.11 to 1.17 atm. The effects of the residence time can be checked by using the third data of which the range is from 3.4 to 4.4 hr. The last data set shows the effects of combinations of reactor conditions with pressure and residence time on behaviors of the reactor. In this set the range of pressure is from 1.14 to 1.24 atm and that of the residence time from 3.5 to 4.0 hr. For the simulation, it is assumed that all the water vaporized from the esterification reactor is removed by using the distillation column and all EG vaporized is recycled. In addition, we consider that extra EG is introduced into the reactor as a mixture with catalysts. This assumption causes a

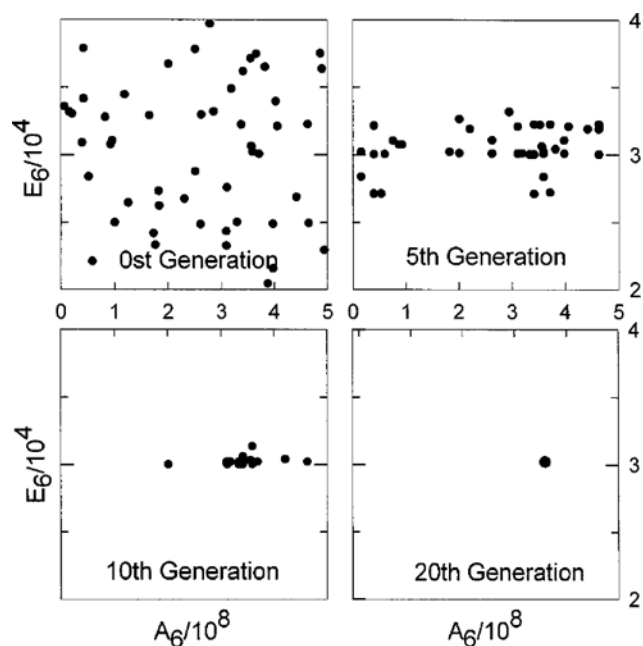


Fig. 4. Population at various generation numbers using GA in the present study

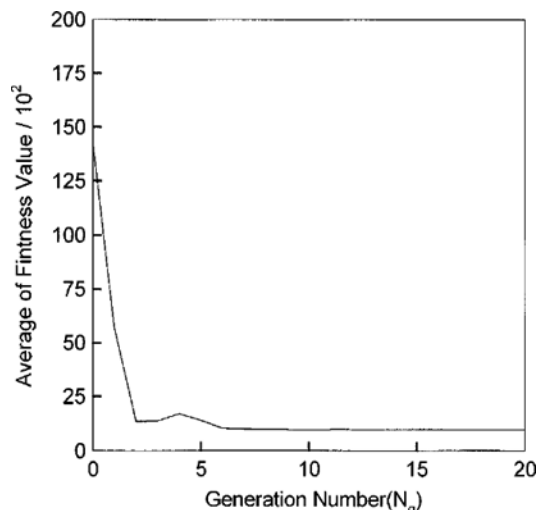


Fig. 5. The degree of convergence in the procedure of optimization.

slight increase of the total EG in the feed.

1. Identification of Reaction Parameters

Data sets from 1 to 3 in Table 5 were used first in the optimization process for the identification of kinetic parameters. The parameters governing selection, crossover and mutation in the genetic algorithm are specified as shown in Table 4. Within 20 generations the genetic algorithm had produced a pair of values for A_6 and E_6 with good convergence. The calculated values of parameters were

$$A_6 = 3.59130 \times 10^8 \text{ and } E_6 = 3.02219 \times 10^4$$

Fig. 4 represents the distribution of population at each generation number. From Fig. 4, we can see that as the generation number increases, the searching space of E_6 approaches an optimum solution faster than that of A_6 . Fig. 5 shows the degree of convergence during the GA computation. The reactor properties achieved by using these parameters are compared with actual plant data sets in Table 5. The vapor flow rates of EG and water (F_{EG}^v , F_w^v) were represented as dimensionless variables for convenience with respect to the flow rate of TPA as well as the concentration of acid end groups in products (C_{acid}^o) with respect to the concentration of TPA in the feed.

The tabulated values have been specified to a high degree of accuracy to highlight the excellent agreement between the calculated and measured reactor properties. Especially, it should be emphasized that the agreement between the calculated and measured data is evident not only in the 1st-3rd data sets but also in the 4th data set. The 4th data set represents the effects of combination between pressure and residence time and was not used in the calculation of the reaction rate parameters. This fact demonstrates that the model developed in the present study can be used to describe the behavior of the actual reactor effectively.

2. Steady-state Reactor Behaviors According to Various Operating Conditions

Simulations have been performed to study the effects of various operating conditions on the conversion and the concentration of acid end groups, on vapor flow rates of EG and water, on the degree of polymerization and concentration of oligomer and on the concentration of DEG and water. In simulations extra EG which is intro-

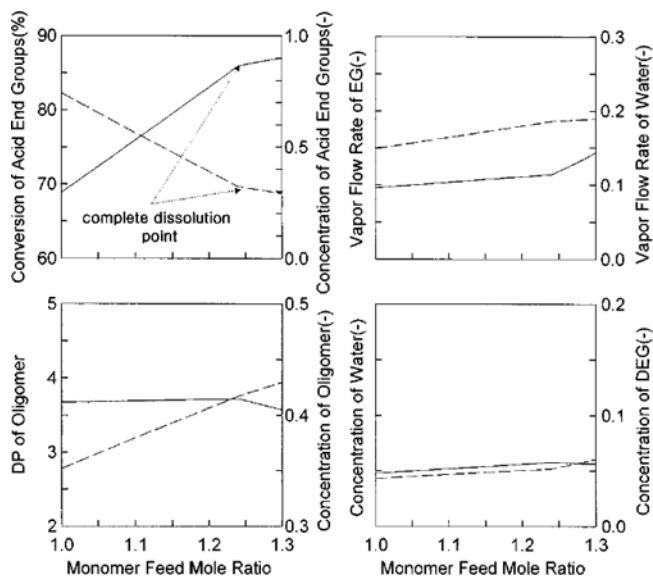


Fig. 6. The effects of monomer feed mole ratio on the reactor performance (left axis: solid lines, right axis: dotted lines).

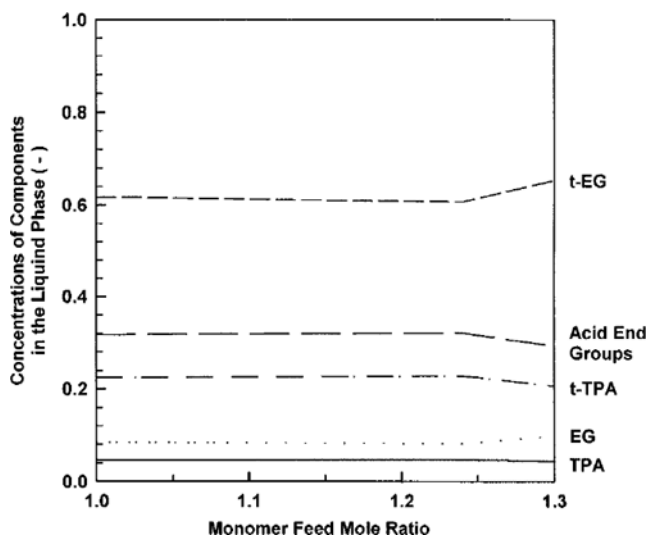


Fig. 7. The concentrations of the components in the liquid phase according to the monomer feed ratios.

duced into the feed mixed with catalysts is not considered and only one operating condition is changed at each simulation while others are fixed at their reference values. Typical steady-state operation conditions of $T=260\text{ }^{\circ}\text{C}$, $P=1.2\text{ atm}$, $a=1.24$, and $\tau=4\text{ hr}$ were used as the reference state. As before, all results were represented as dimensionless groups for convenience.

Figs. 6 and 7 show the effects of the monomer feed mole ratio on the various reactor behaviors and product properties. It should be noticed that the bent parts on the line is the complete dissolution point. The complete dissolution point is where the concentration of solid TPA is zero. In Fig. 7 the concentrations of components in the liquid phase of the reaction mixtures are kept nearly constant until the complete dissolution of TPA. This is due to the balance between more dissolved TPA in liquid phase with additional EG and the increase in the degree of reactions. Namely, the use of large

quantity of EG is useful to enhance the solubility of TPA in the liquid phase. However, the enhanced amount of TPA in the liquid phase by larger amount of EG accelerates the consumption reactions of TPA and EG by catalysis of the acid end groups in the reactions. Therefore, when the monomer feed ratio increases, the total concentration of acid end groups in the reaction mixtures decreases (the conversion of acid end groups increases), since solid TPA has to be provided into the liquid phase continuously and the consumption of TPA by reactions increases. The EG vapor flow rate is not changed too much, and more water is vaporized because reaction products are increased with the increment of the monomer feed mole ratio. The degree of polymerization is also kept constant and the concentration of oligomer continues to be increased. This means that the increment of the monomer feed mole ratio causes increase of the concentration of oligomer while the chain length of oligomer is not changed.

After the complete dissolution of TPA, the concentration of acid end groups in the liquid phase decreases with the increment of the monomer feed ratio because dissoluble TPA into the liquid phase does not exist any more and the proceeding reactions continuously consume TPA in the liquid phase. For this reason, the degree of esterification reaction is lessened suddenly after the complete dissolution of TPA. Furthermore, the reverse reaction of polycondensation reaction becomes predominant as the amount of remaining EG increases. This causes the concentration of acid end groups in the reaction mixtures to reduce sluggish behavior (the growth rate of the conversion of acid end groups becomes sluggish as well) and the amount of water vaporized to be decreased while the concentration of oligomer increases but its chain length decreases and the DEG formation reaction occurs more actively with the increment of the excess EG.

Fig. 8 shows the effect of the reaction temperature on typical variables. Increase of the reaction temperature results in the enhanced solubility of TPA and the reaction rate, both of which depend on only temperature at the operating conditions considered in the present

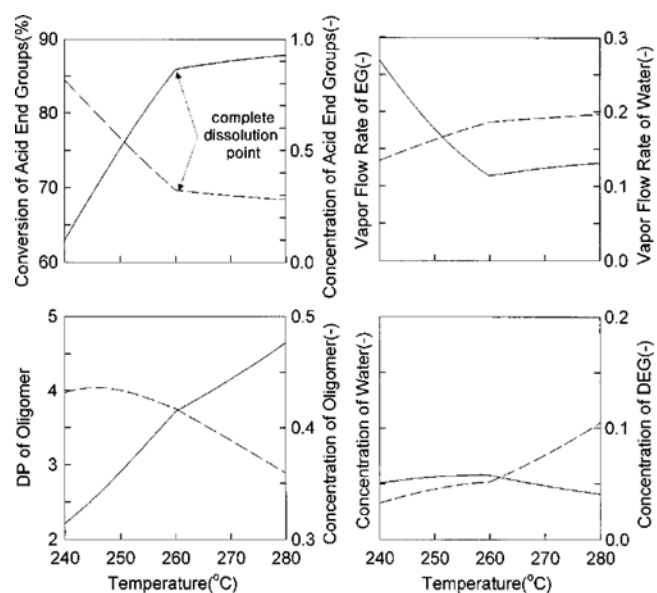


Fig. 8. The effects of reaction temperature on the reactor performance (left axis: solid lines, right axis: dotted lines).

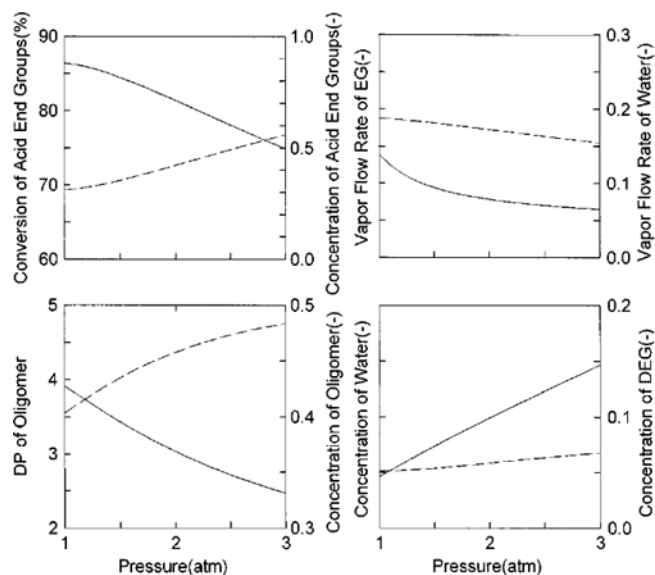


Fig. 9. The effects of pressure on the reactor performance (left axis: solid lines, right axis: dotted lines).

study. Therefore, the concentration of acid end groups decreases and that of DEG increases as the reaction temperature increases. But the amount of vaporized EG decreases distinctly according to the monomer feed ratio. It is due to the fixed quantity of EG though the reaction rate rises when the reaction temperature increases. Without being affected by the monomer feed ratio, DP increases as much as the decreased concentration of oligomer. This implies that the increasing rate of the chain length in oligomer molecules becomes much faster than that of the new oligomer production reaction with increasing reaction temperature. After the complete dissolution EG vapor increases because of unreacted excess EG with TPA. It is interesting to note that the concentration of water decreases and that of DEG increases abruptly. This is because the esterification reactions are restrained and the reactions involving only EG groups are promoted with the increment of the reaction temperature after the complete dissolution.

The effects of the reaction pressure are shown in Fig. 9. When the reaction pressure is increased at different operating conditions, the flow rates of EG and water vapor decrease and their concentrations in the reaction mixtures increase. Consequently, the effects of increasing pressure are equivalent to those of increasing EG and water in the reaction mixtures. EG and water not only promote reverse reactions due to the increased amount of by-products but also lead the esterification reaction to forward direction due to the increased solubility of TPA. However, because the promotion of forward reactions in esterification by more dissolved TPA is less than that of reverse reactions, all indexes about reaction efficiency decrease with increasing pressure except the efficiency rising by decreasing vapor flow rates. Hence, it is advantageous to operate the reactor at low pressure.

Fig. 10 shows the dependency of the reactor performance on the residence time changing from 3 to 5 hr. The increase of the residence time leads the solubility of TPA to increase and consequently to reach the complete dissolution point. The effects of the residence time are similar to the case of increasing reaction tempera-

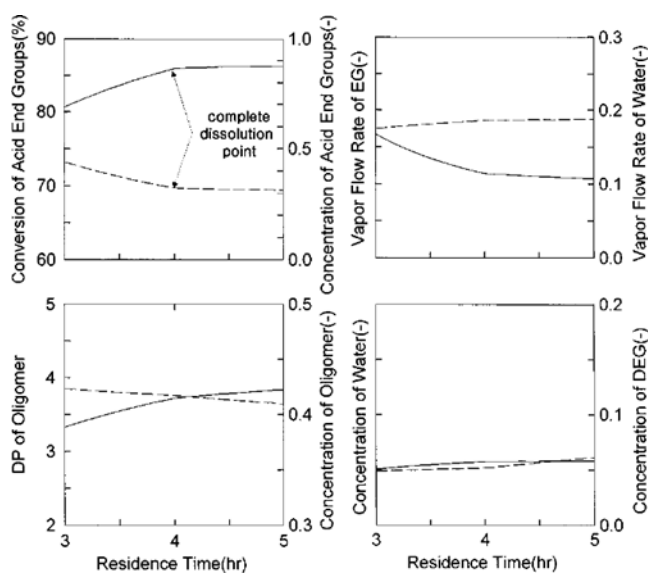


Fig. 10. The effects of residence time on the reactor performance (left axis: solid lines, right axis: dotted lines).

ture although not so sensitive.

When Figs. 6-10 are considered simultaneously, the effects of each feed condition on the reactor performance can be summarized as follows: the increment of the monomer feed mole ratio and temperature results in better reactor performance as well as increased degrees of entire reactions. But after complete dissolution of solid TPA, the increasing rate of the conversion of acid end groups slows down, the concentration of DEG increases while DP decreases and vapor flow rates increase. This fact indicates that excess EG and higher temperature after the complete dissolution of TPA should be avoided to maintain optimality, although excess EG and higher temperature are useful to increase the conversion. The increment of pressure deteriorates the reactor performance and promotes the inversion reaction, while vapor flow rates decrease within the narrow range. From these facts we can see that pressure should be maintained as low as possible. Increasing residence time is also important to increase the reactor performance. But increased residence time causes a decrease of the conversion of acid end groups, increase of the concentrations of by-products, and slow down of the increase rate of DP until TPA is completely dissolved. These results on the reactor behaviors remind us that the condition of complete dissolution of TPA is the most important factor in the analysis and optimization of the esterification reactor.

CONCLUSIONS

In this study, an improved model for a continuous direct esterification reactor was developed by using a genetic algorithm. The optimization method based on the genetic algorithm was used to calculate the rate parameters of DEG formation reaction based upon actual operation data with various ranges. Results of simulations showed good agreement with actual operation data. This indicates that the reaction rate parameters can be successfully identified by using a genetic algorithm and plant data. The effects of key operating variables (temperature, pressure, feed mole ratio and residence

time) on the reactor performance were investigated. It was observed that the reactor performance strongly depends on the degree of dissolution of the solid TPA in the reaction mixtures.

NOMENCLATURE

a	: monomer feed mole ratio
A_i	: frequency factor for reaction i [(kg/mol) ² /min]
C	: concentration [mol/kg]
C_{acid}	: concentration of acid end groups in the liquid phase ($2C_{TPA} + C_{1-TPA}$) [mol/kg]
C_{acid}^o	: concentration of acid end groups in the reaction mixtures ($2C_{TPA}^o + C_{1-TPA}^o$) [mol/kg]
C_p	: heat capacity [kcal/(kg·K)]
Conversion	: conversion of acid end groups [%]
DP	: degree of polymerization
E	: error function
E_i	: activation energy [cal/mol]
F	: flow rate [kg/min]
I	: objective function
k	: effective kinetic constant [kg/(mol·min)]
K_i	: equilibrium constant for reaction i
l_{chrom}	: chromosome length
Max_{gen}	: maximum generation number
n	: mole number [mol]
N_d	: the number of decision variables
N_g	: generation number
N_p	: population size
\mathbf{P}	: vector of product properties
P_c	: crossover operator
P_m	: mutation operator
R	: ideal gas constant [1.987 cal/mol·K]
R_i	: reaction rate for reaction i [mol/kg·min]
seed	: random seed
t	: time [min]
T	: absolute temperature [K]
W	: weight of liquid phase in the reaction mixtures [kg]
W_{mix}	: weight of reaction mixtures [kg]
\mathbf{x}	: vector of reaction rate parameters
x	: mole fraction in the liquid phase of the reaction mixtures
y	: mole fraction in the vapor phase of the reaction mixtures
(-)	: dimensionless

Greek Letters

α	: solubility of solid TPA in the reaction mixtures [mol/kg]
τ	: residence time [hr]
ρ	: density of the reaction mixtures [kg/ λ]
ω	: weight fraction

Superscripts

i	: input
r	: reference case
R	: reflux
o	: output

v	: vapor
s	: solid phase
l	: liquid phase
sat	: saturated

Subscripts

mix	: reaction mixtures
calc	: calculated value
plant	: original plant data value
T	: total
acid	: acid end groups
OLG	: oligomer

REFERENCES

- Bhaskar, V., Gupta, S. K. and Ray, A. K., "Simulation of an Industrial Finishing-Stage Polycondensation Reactor in the Poly(ethylene terephthalate) Manufacture," The 8th APCCHE Congress, Seoul, Korea, 59 (1999).
- Besnoin, J. M. and Choi, K. Y., "Identification and Characterization of Reaction Byproducts in the Polymerization of Polyethylene Terephthalate," *J. Macromol. Sci. Rev. Macromol. Chem. Phys.*, **29**(1), 55 (1989).
- Davis, L., "Genetic Algorithms and Simulated Annealing, Morgan Kaufmann," Morgan Kaufmann, San Mateo, CA (1987).
- Deb, K., "Optimization for Engineering Design: Algorithms and Examples," Prentice-Hall of India, New Delhi (1996).
- Flory, P. J., "Principles of Polymer Chemistry," 1st ed., Cornell University Press, Ithaca, New York (1953).
- Goldberg, D. E., "Genetic Algorithms in Search, Optimization and Machine Learning," Addison-Wesley, Reading, MA (1989).
- Harris, S. D., Elliott, L., Ingham, D. B., Pourkashanian, M. and Wilson, C. W., "The Optimization of Reaction Rate Parameters for Chemical Kinetic Modeling of Combustion using Genetic Algorithms," *Comput. Methods. Appl. Mech. Engrg.*, **190**, 1065 (2000).
- Holland, J. H., "Adaptation in Natural and Artificial Systems," University of Michigan Press, Ann Arbor (1975).
- Hovenkamp, S. G. and Munting, J. P., "Formation of Diethylene Glycol as a Side Reaction during Production of Polyethylene of Polyethylene Terephthalate," *J. Polym. Sci. Part A-1*, **8**, 679 (1970).
- Immanuel, C. D. and Gupta, S. K., "Optimization of the First Stage Continuous Reactor-Sequence in Polyester Manufacture from Purified Terephthalic Acid," *J. Polym. Eng.*, **20**(1), 51 (2000).
- Kang, C. K., Lee, B. C., Ihm, D. W. and Tremblay, D. A., "A Simulation Study on Continuous Direct Esterification Process for Poly(ethylene terephthalate) Synthesis," *J. Appl. Polym. Sci.*, **63**, 163 (1997).
- Krevelen, D. W. van., "Properties of Polymers," Elsevier, New York, 3rd ed., 109 (1990).
- Kumar, A., Sharma, S. N. and Gupta, S. K., "Optimization of the Polycondensation Stage of Poly(ethylene terephthalate) Reactors," *J. Appl. Polym. Sci.*, **29**, 1045 (1984).
- Michalewicz, Z., "Genetic Algorithms+Data Structures=Evolution Programs," Springer, Berlin, 3rd ed. (1996).
- Ottou, J. and Ratton, S., "Investigation of the Formation of Poly(ethylene terephthalate) with Model Molecule: Kinetics and Mechanism of the Catalytic Esterification and Alcoholysis Reactions," *J. Polym. Sci.*, **26**, 2183 (1998).

- Park, T. Y. and Froment, G. F., "A Hybrid Genetic Algorithm for the Estimation of Parameters in Detailed Kinetic Models," *Comp. Chem. Eng.*, **22**, s103 (1998).
- Polifke, W., Geng, W. and Döbbling, K., "Optimization of Rate Coefficients for Simplified Reaction Mechanisms with Genetic Algorithms," *Combustion and Flame*, **113**, 119 (1998).
- Ravindranath, K. and Mashelkar, B. A., "Modeling of Poly(ethylene terephthalate) Reactors: 4. A Continuous Esterification Process," *Polym. Eng. and Sci.*, **22**(10), 610 (1982).
- Ravindranath, K. and Mashelkar, B. A., "Polyethylene Terephthalate I. Chemistry, Thermodynamics and Transport Properties," *Chem. Eng. Sci.*, **41**(9), 2197 (1986).
- Reimschuessel, H. K., Debona, B. T. and Murthy, A. K. S., "Kinetics and Mechanism of the Formation of Glycol Esters: Benzoic Acid-Ethylene Glycol System," *J. Polym. Sci.*, **17**, 3217 (1979).
- Yamada, T., "A Mathematical Model for a Continuous Esterification Process with Recycle Between Terephthalic Acid and Ethylene Glycol," *J. Appl. Polym. Sci.*, **45**, 1919 (1992).
- Yamada, T., Imamura, Y. and Makimura, O., "A Mathematical Model for Computer Simulation of a Direct Continuous Esterification Process Between Terephthalic Acid and Ethylene Glycol: Part 1. Model Development," *Polym. Eng. and Sci.*, **25**(12), 788 (1985).
- Yeo, Y. K., Cho, H. J., Park, W. H. and Moon, B. K., "Modeling and Simulation of a Wet Hemihydrate Phosphoric Acid Process," *Korean J. Chem. Eng.*, **13**, 585 (1996).
- Yeo, Y. K., Choo, J. O., Kim, M. K., Kim, K. S. and Chang, K. S., "Modeling and Simulation of a Sulfolane Extraction Process," *Korean J. Chem. Eng.*, **15**, 90 (1998).
- Wolf, D. and Moros, R., "Estimating Rate Constants of Heterogeneous Catalytic Reactions Without Supposition of Rate Determining Surface Steps-An Application of a Genetic Algorithm," *Chem. Eng. Sci.*, **52**(7), 475 (1997).